

WCAP-17942-NP (APR1400-A-M-NR-14001-NP)  
Revision 3

July 2017

# **KHNP APR1400 Flywheel Integrity Report**

**WCAP-17942-NP (APR1400-A-M-NR-14001-NP)**  
**Revision 3**

**KHNP APR1400 Flywheel Integrity Report**

**Gordon Z. Hall\***  
MRCDA – I, Engineering Services

**July 2017**

Reviewer: Thomas E. Demers\*  
MRCDA – I, Engineering Services

Approved: Patrick Hill for Carl J. Gimbrone\*, Manager  
MRCDA – I, Engineering Services

\*Electronically approved records are authenticated in the electronic document management system.

---

Westinghouse Electric Company LLC  
1000 Westinghouse Drive  
Cranberry Township, PA 16066, USA

© 2017 Westinghouse Electric Company LLC  
All Rights Reserved

## ABSTRACT

This report demonstrates that the APR1400 reactor coolant pump (RCP) flywheel satisfies all of the RCP flywheel integrity criteria of the design specification [1] and U.S. NRC Regulatory Guide 1.14 [2]. The combination of shrink-fit and rotational stresses at normal pump operation speed and at overspeed are calculated and shown to be acceptable with respect to the prescribed criteria in [1, 2, and 8].

The critical speeds for ductile and non-ductile fracture are computed and shown to be significantly greater than two times normal speed as required by the Regulatory Guide [2]. It is demonstrated that excessive deformation will not result from an overspeed condition.

## TABLE OF CONTENTS

ABSTRACT.....	ii
LIST OF TABLES .....	iv
LIST OF FIGURES .....	iv
1 BACKGROUND AND PURPOSE .....	1-1
2 REQUIREMENTS.....	2-1
2.1 LIMITS OF APPLICABILITY.....	2-1
2.2 OPEN ITEMS.....	2-1
2.3 DISCUSSION OF SIGNIFICANT ASSUMPTIONS .....	2-1
2.4 ACCEPTANCE CRITERIA .....	2-1
3 METHODOLOGY .....	3-1
3.1 STRESSES AND RADIAL DISPLACEMENT DUE TO SHRINK FIT OF SECTIONS OF FLYWHEEL .....	3-1
3.2 STRESSES AND RADIAL DISPLACEMENT DUE TO ROTATION OF FLYWHEEL.....	3-2
3.3 STRESS INTENSITY FACTOR OF ASSUMED CRACK IN FLYWHEEL .....	3-3
4 INPUT.....	4-1
4.1 MATERIALS .....	4-1
4.2 GEOMETRY .....	4-1
4.3 ROTATIONAL SPEEDS PER THE DESIGN SPECIFICATION.....	4-2
5 EVALUATION AND ANALYSIS .....	5-1
5.1 SHRINK FIT REQUIREMENTS.....	5-1
5.2 HUB-WHEEL ASSEMBLY SHRINK FIT CONTACT PRESSURE .....	5-1
5.3 HUB-WHEEL ASSEMBLY SHRINK FIT STRESSES.....	5-2
5.4 ATTACH TO SHAFT SHRINK FIT CONTACT PRESSURE .....	5-2
5.5 ATTACH TO SHAFT SHRINK FIT STRESSES.....	5-2
5.6 STRESSES DUE TO ROTATION AT 1,200 RPM.....	5-4
.....	5-6
5.7 STRESSES DUE TO ROTATION AT 125% OVER SPEED, 1,500 RPM .....	5-6
5.8 STRESS DUE TO ROTATION AT 1,800 RPM .....	5-6
5.9 JOINT RELEASE SPEED FOR PRESCRIBED SHRINK VALUES .....	5-7
5.10 CONSIDERATION OF MINIMUM SHRINK FIT.....	5-7
5.11 EVALUATION OF STRESSES .....	5-8
5.12 CONSIDERATION OF SEISMIC EVENT.....	5-8
5.13 STRESS INTENSITY FACTOR OF CRACK FOR OUTER WHEEL .....	5-8
5.14 EVALUATION OF INTEGRITY .....	5-13
5.15 FATIGUE CRACK GROWTH.....	5-14
6 RESULTS AND CONCLUSIONS .....	6-1
7 REFERENCES .....	7-1



## LIST OF TABLES

Table 5-1: Normal and Critical Speed Comparison .....	5-14
---	------

## LIST OF FIGURES

Figure 4-1: APR1400 Flywheel Sketch [6] .....	4-2
Figure 5-1: Standstill Stress due to Wheel Assembly Shrink Fit .....	5-2
Figure 5-2: Standstill Stress due to Shrink Fit onto Shaft .....	5-3
Figure 5-3: Total Stress at Standstill .....	5-3
Figure 5-4: Stress due to Rotation at 1,200 RPM .....	5-4
Figure 5-5: Total Stress at 1,200 RPM .....	5-5
Figure 5-6: Total Stress at Operation at 1,500 RPM .....	5-6
Figure 5-7: Total Stresses at Joint Release Speed of 1,786 RPM .....	5-7
Figure 5-8: Polynomial Tangential Stress at Standstill .....	5-10
Figure 5-9: Stress Intensity Factor versus Crack Length at Standstill .....	5-10
Figure 5-10: Polynomial Tangential Stress at 1,200 RPM .....	5-11
Figure 5-11: Stress Intensity Factor versus Crack Length at 1,200 RPM .....	5-11
Figure 5-12: Polynomial Tangential Stress at 1,500 RPM .....	5-12
Figure 5-13: Stress Intensity Factor versus Crack Length at 1,500 RPM .....	5-12
Figure 5-16: Rotation Speed to Reach a $K_{IC}$ of 150 ksi-in <sup>1/2</sup> .....	5-13
Figure 5-17: Change in Outer Wheel $K_I$ from Standstill to Normal Operation .....	5-15

# 1 BACKGROUND AND PURPOSE

In support of the Design Certification Application (DCA) of the APR1400 Advanced Light Water Reactor (ALWR) design, Korea Hydro & Nuclear Power (KHNP) requested Westinghouse to evaluate the integrity of the APR1400 RCP motor flywheel design. The subject matter of this report is the flywheel integrity analyses performed by Westinghouse to quantify the structural integrity of the flywheel as well as the critical speeds of the flywheel under normal and off-normal operating conditions. Specifically, the objective of the analyses is to compute the stresses and critical speeds and to compare the results to criteria in the design specification [1] and U.S. NRC Regulatory Guide 1.14 [2].

Portions of this report contain proprietary information. Proprietary information is identified and bracketed. For each of the bracketed sections, the reasons for the proprietary classification are provided using superscripted letters “a”, “c”, and “e”. These letters stand for:

- a. The information reveals the distinguishing aspects of a process or component, structure, tool, method, etc. The prevention of its use by Westinghouse’s competitors, without license from Westinghouse, gives Westinghouse a competitive economic advantage.
- c. The information, if used by a competitor, would reduce the competitor’s expenditure of resources or improve the competitor’s advantage in the design, manufacture, shipment, installation, assurance of quality, or licensing of a similar product.
- e. The information reveals aspects of past, present, or future Westinghouse- or customer-funded development plans and programs of potential commercial value to Westinghouse.

Revision 1 corrects wording in Section 5.11 in response to CAPAL 100377490. This correction has no impact on any of the evaluations, results, or conclusions in this report. Revision 1 also details the critical speed for excessive deformation discussion in Section 6, item 9.

Revision 2 changes the Section 2.4, acceptance criterion 1 stress limit to  $1/3 S_y$  from  $1/3 S_u$  (Revisions 0 and 1) for total stress in the flywheel at standstill and normal operating speed. The measured  $S_y$  is conservatively assumed to be 800 MPa or 116,030 psi. Preliminary measured  $S_y$  is 816 MPa per [9], and is pending on confirmation by Siemens’ material test report.

Revision 3 updates all calculations per the updated design specification [1] which removed the previous standstill stress in criterion 1, and the joint release speed and stress requirements in criterion 3 in previous revisions. The minimum specified yield strength,  $S_y = 640$  MPa (92,824 psi) is used instead of the preliminary measured  $S_y$  value reported in [9]. Shrink fit dimensions are optimized to meet the normal operating stress limit of  $1/3 S_y$ . The previous revisions considered shrink fit reduction based on radial displacement delta of the shaft, hub and outer wheel as individual pieces. At the same time, the rotation inertia stress assumed the hub and outer wheel as one solid piece. This method resulted in a conservative total stress. Revision 3 considers the shrink fit stress at standstill, and combines the rotation inertia stress with the shaft, hub and outer wheel as a single piece. Detail discussion is in Section 5.6. All affected calculation results are updated. The terms “hoop stress” and “tangential stress” are used interchangeably in this revision.



## **2 REQUIREMENTS**

### **2.1 LIMITS OF APPLICABILITY**

This report is applicable to the KHNP APR1400 flywheel only.

### **2.2 OPEN ITEMS**

This report contains no open items.

### **2.3 DISCUSSION OF SIGNIFICANT ASSUMPTIONS**

This report contains no significant assumptions.

### **2.4 ACCEPTANCE CRITERIA**

The acceptance criteria in the specification [1] and the standard review plan (SRP) [8] include:

1. The total stress in the flywheel at normal operating speed does not exceed 1/3 of the minimum specified or measured yield strength ( $1/3 S_y$ ) per [1 and 8].
2. The total stress at design overspeed does not exceed 2/3 of the minimum specified or measured yield strength ( $2/3 S_y$ ), where design overspeed is 125% of normal operating speed.

The Regulatory Guide acceptance criteria are established in [2] as:

3. Flywheel assembly should be designed to withstand normal conditions, anticipated transients, the design basis LOCA, and the safe shutdown earthquake without loss of structural integrity.
4. The critical speed for ductile fracture should be predicted.
5. The critical speed for non-ductile fracture should be predicted.
6. The normal speed should be less than one-half of the lowest critical speeds.
7. The predicted LOCA overspeed should be less than the lowest critical speeds.
8. The critical speed for excessive deformation of the flywheel should be predicted.

### 3 METHODOLOGY

This analysis calculates the stresses in the flywheel resulting from the shrink fit of the sections of the flywheel and the rotation of the flywheel at various speeds. Using these stresses, the integrity of the flywheel is evaluated by assuming a crack in the highest stressed location of the flywheel to assess if the criteria of [1] and [2] are satisfied.

#### 3.1 STRESSES AND RADIAL DISPLACEMENT DUE TO SHRINK FIT OF SECTIONS OF FLYWHEEL

The stresses due to shrink fit are determined by the formulae [3, page 683].

The flywheel is constructed by shrink fitting three parts. First, the outer wheel is shrink fitted to the hub. Next, the assembly of the outer wheel and hub is shrink fitted to the shaft. Then, the amount of shrink fit required to maintain contact between the outer wheel and the shaft is determined by the relative radial displacement due to rotation at the maximum rotational speed.

The following definitions apply:

a = outside radius of outer wheel

b = inner radius of outer wheel

c = outer radius of the hub, nominally equal to b

d = averaged inner radius of hub

e = outer radius of the shaft, nominally equal to d

The relationship between radial displacement of the inner radius and contact pressure for the outer wheel is expressed as:

$$\Delta b = (Pb/E)[(a^2 + b^2)/(a^2 - b^2) + \nu] \quad \text{Equation 1 [3]}$$

In Equation 1:

a = outside radius of wheel

b = inside radius of wheel

P = contact pressure between outer wheel and hub

E = Young's modulus

$\nu$  = Poisson ratio

radial stress:

$$S_r = -Pb^2(a^2 - r^2)/[r^2(a^2 - b^2)] \quad \text{Equation 2 [3]}$$

In Equation 2:

r = distance from center of wheel

P = pressure on inner radius of wheel



tangential stress:

$$St = Pb^2(a^2 + r^2)/[r^2(a^2 - b^2)] \quad \text{Equation 3 [3]}$$

The relationship between the radial displacement of the outer radius and the contact pressure for the hub is expressed as:

$$\Delta c = -(Pc/E)[(c^2 + d^2)/(c^2 - d^2) - \nu] \quad \text{Equation 4 [3]}$$

In Equation 4:

c = outside radius of hub

d = averaged inside radius of hub

radial stress:

$$Sr = -Pc^2(r^2 - d^2)/[r^2(c^2 - d^2)] \quad \text{Equation 5 [3]}$$

In Equation 5:

r = distance from center of wheel

P = pressure on outer radius of hub

tangential stress:

$$St = -Pc^2(d^2 + r^2)/[r^2(c^2 - d^2)] \quad \text{Equation 6 [3]}$$

### 3.2 STRESSES AND RADIAL DISPLACEMENT DUE TO ROTATION OF FLYWHEEL

The stresses and displacements due to rotation of a disk of uniform thickness are taken from [3, page 746].

The change in the inner radius of the outer wheel due to rotation of “W” in radians/sec is expressed as:

$$\Delta b = (1/4)(\text{density/gravity}) * W^2 * (b/E) * [(3 + \nu)a^2 + (1 - \nu)b^2] \quad \text{Equation 7 [3]}$$

The change in the outer radius of the hub due to rotation of “W” in radians/sec is expressed as:

$$\Delta c = (1/4)(\text{density/gravity}) * W^2 * (c/E) * [(1 - \nu)c^2 + (3 + \nu)d^2] \quad \text{Equation 8 [3]}$$

Equations 7 and 8 are used to calculate shrink fit values.

The general forms for tangential and radial stress due to rotation are:

$$S_t = (1/8)(\text{density/gravity}) * W^2 * [(3 + \nu) * (R_o^2 + R_i^2 + R_o^2 R_i^2 / r^2) - (1 + 3\nu)r^2]$$

$$S_r = (1/8) * (3 + \nu) * (\text{density/gravity}) * W^2 * [R_o^2 + R_i^2 - (R_o^2 R_i^2 / r^2) - r^2]$$

where,  $R_i$  is inner radius;  $R_o$  is outer radius; “ $r$ ” is the radial location of the stress.

The shaft, hub and outer wheel rotate as a solid piece until separation, therefore,  $R_i$  for whole assembly including the shaft is zero. The equations for tangential and radial stresses become:

$$S_t = (1/8)(\text{density/gravity}) * W^2 * [(3 + \nu) * a^2 - (1 + 3\nu)r^2] \text{ Equation 9 [3]}$$

$$S_r = (1/8) * (3 + \nu) * (\text{density/gravity}) * W^2 * (a^2 - r^2) \text{ Equation 10 [3]}$$

### 3.3 STRESS INTENSITY FACTOR OF ASSUMED CRACK IN FLYWHEEL

The stress intensity factor for an axial crack in a cylinder will be used to compute the effect of a crack in the outer wheel. The highest stress location is the inner radius of the outer wheel. The stress intensity factor formula is taken from [4, Section C.5.5]. This formula computes the stress intensity factor for a fourth order polynomial stress distribution for a longitudinal (axial) inside surface crack on a cylinder of infinite length. The tabular coefficients in [4] are listed up to a thickness to inside radius ratio ( $t/R_i$ ) of 1.0.

$$\left( \begin{array}{l} \\ \\ \\ \\ \end{array} \right) \quad \text{a, c, e}$$

$$S_t = S_0 + S_1(x/t) + S_2(x/t)^2 + S_3(x/t)^3 + S_4(x/t)^4 \quad \text{Equation 11}$$

$$K_I = [G_0 S_0 + G_1 S_1(a/t) + G_2 S_2(a/t)^2 + G_3 S_3(a/t)^3 + G_4 S_4(a/t)^4] \sqrt{(\pi a)} \quad \text{Equation 12}$$

In Equations 11 and 12:

$S_t$  = tangential stress

$a$  = radial dimension of assumed crack

$t$  = distance between inner and outer radii of wheel

$x$  = distance from cracked edge

## 4 INPUT

The units of dimensions and material properties are given in metric units. The calculations are performed in customary U.S. units. Some metric units will be stated as reference values for comparison with other flywheel documentation.

The stress analysis in [6] is performed in metric units. The results of the analysis in [6], when converted to customary U.S. units, are slightly different than the results calculated herein (where the input values are converted from metric units).

### 4.1 MATERIALS

The material selected for both parts of the flywheel is 26NiCrMoV14-5 [6]. This report uses the stated properties in [6]. The fracture toughness will be confirmed by direct test method per SRP [8].

The modulus of elasticity (E) is 204,000 MPa or 29,587,956 psi.

The minimum  $S_y = 640$  MPa,  $1/3 S_y = 213$  MPa or 30,941 psi;  $2/3 S_y = 427$  MPa or 61,883 psi.

The minimum tensile strength ( $S_u$ ) is 800 MPa or 116,030 psi.  $0.7 S_u = 560$  MPa or 81,221 psi.

The normal operating temperature is conservatively assumed to be the environment condition, 49°C to 10°C, or 120°F to 50°F [1].

The minimum fracture toughness,  $K_{IC}$ , at normal operating temperature is at least 165 MPa-m<sup>1/2</sup> or 150 ksi-in<sup>1/2</sup> [1].

The density of the flywheel material is 7,850 kg/m<sup>3</sup> or 0.283 lbs/in<sup>3</sup>.

### 4.2 GEOMETRY





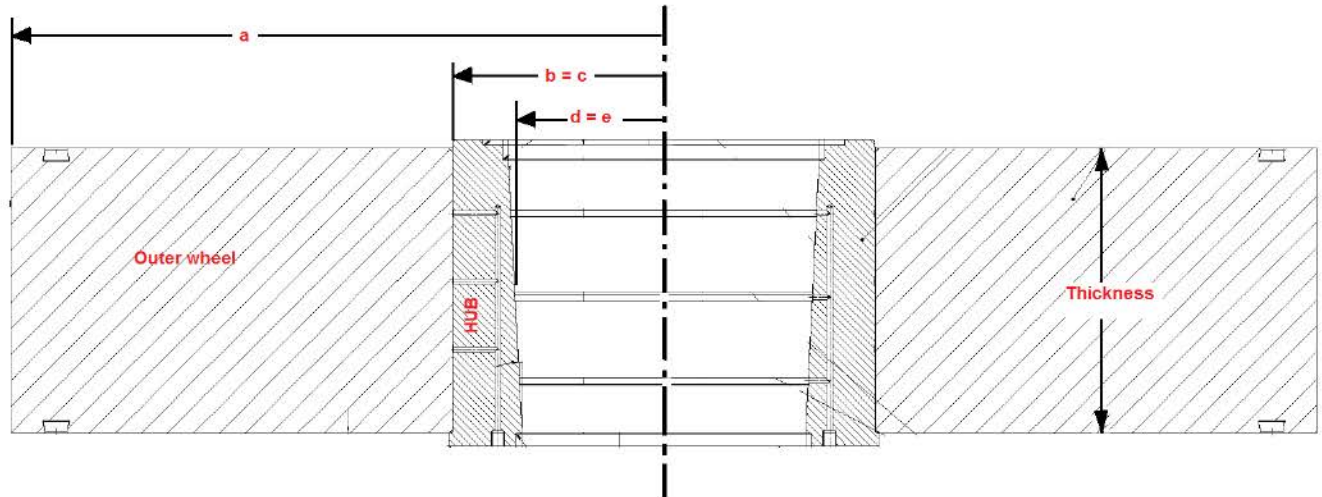


Figure 4-1: APR1400 Flywheel Sketch [6]

### 4.3 ROTATIONAL SPEEDS PER THE DESIGN SPECIFICATION

The speeds that are to be addressed include:

- normal operation at 1,200 RPM
- 125% of normal operation = 1,500 RPM
- loss of shrink fit
- critical speed for ductile fracture
- critical speed for non-ductile fracture
- critical speed for excessive deformation



## 5 EVALUATION AND ANALYSIS

### 5.1 SHRINK FIT REQUIREMENTS

The shrink fit is optimized based on the predicted separation speed of 1,680 RPM. The normal operation stress is confirmed to satisfy the criterion of  $1/3 S_y$  with the optimized shrink fit. For this analysis, the manufacturing tolerances and smoothing tolerances listed below are assumed. Note that the prescribed tolerance values are with respect to the diameter. The minimum manufacturing tolerances are zero; the smoothing tolerances were considered to be either positive or negative. The normal operating stress was confirmed to meet the  $1/3 S_y$  criterion using the optimized shrink fit. Maximum tolerances will be used for stress and fracture calculations; minimum tolerances will be used for separation speed calculation only.

- Hub to outer wheel tolerance with respect to diameter
  - Manufacturing = [  $\phantom{0.001}$  ]<sup>a, c, e</sup>
  - Smoothing = [  $\phantom{0.001}$  ]<sup>a, c, e</sup>
- Hub to shaft tolerance with respect to diameter
  - Manufacturing = [  $\phantom{0.001}$  ]<sup>a, c, e</sup>
  - Smoothing = [  $\phantom{0.001}$  ]<sup>a, c, e</sup>
- Hub to outer wheel shrink fit = 0.0123 inch
- Hub to shaft shrink fit = 0.0091 inch

The shrink fit is combined with the tolerance values to determine the total interference for the stress and separation calculations.

The maximum tolerances produce the shrink fits that generate the highest stress:

- Hub to outer wheel shrink fit = 0.01386 inch.
- Hub to shaft shrink fit is 0.01028 inch.

The minimum tolerances produce the shrink fits that generate the lowest separation speed:

- Hub to outer wheel shrink fit = 0.01195 inch.
- Hub to shaft shrink fit is 0.00894 inch.

### 5.2 HUB-WHEEL ASSEMBLY SHRINK FIT CONTACT PRESSURE

First, the outer wheel is shrink fitted on to the hub. The shrink fit contact pressure between the hub and the outer wheel is computed by combining Equation 1 and Equation 4. The shrink fit is:

$$\Delta b - \Delta c = 0.01386 \text{ inches}$$

This results in a contact pressure,  $P = 7,588$  psi.

### 5.3 HUB-WHEEL ASSEMBLY SHRINK FIT STRESSES

The shrink fit stresses in the wheel assembly before attaching to the shaft are computed using Equations 2, 3, 5, and 6, and the contact pressure,  $P = 7,588$  psi.

The stresses as a function of radial position are shown in Figure 5-1.

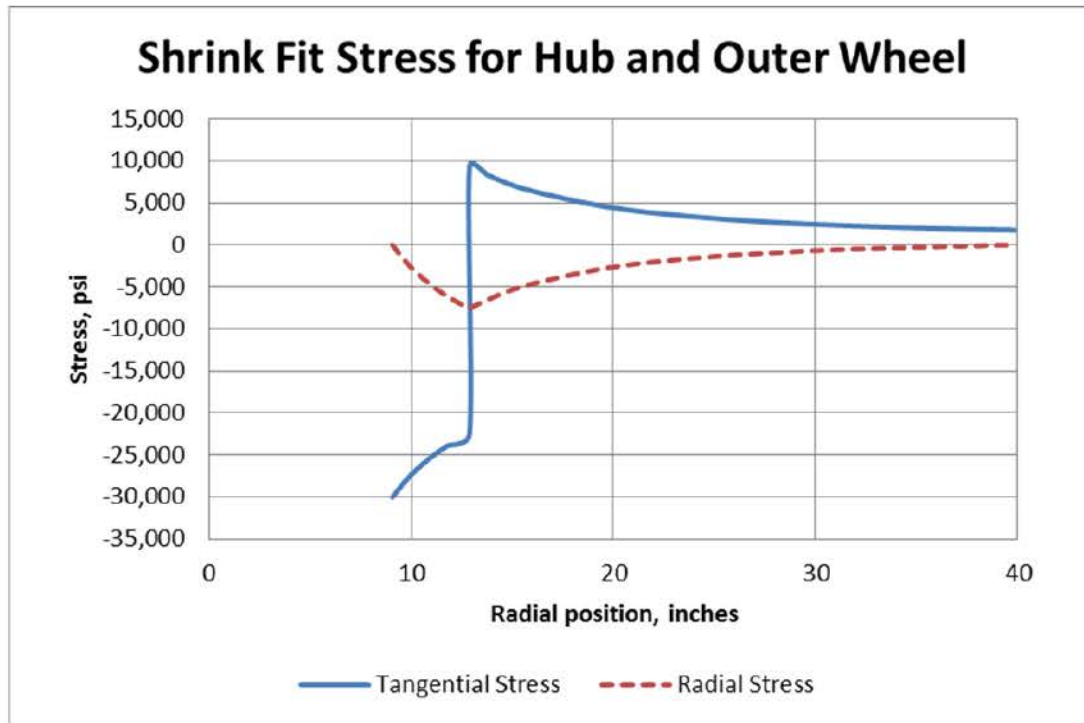


Figure 5-1: Standstill Stress due to Wheel Assembly Shrink Fit

### 5.4 ATTACH TO SHAFT SHRINK FIT CONTACT PRESSURE

The second shrink fit attaches the hub-wheel assembly to the shaft. The contact pressure due to the shrink of the wheel assembly onto the shaft is computed by combining Equation 1 for the wheel assembly and Equation 4 for the shaft:

$$\Delta d - \Delta e = 0.01028 \text{ inches}$$

This results in a contact pressure,  $P = 15,984$  psi.

### 5.5 ATTACH TO SHAFT SHRINK FIT STRESSES

The stresses due to the shrink fit onto the shaft computed by Equation 2, Equation 3, and the contact pressure  $P = 15,984$  psi for the wheel assembly are shown in Figure 5-2. These stresses are added to the shrink fit stresses due to the assembly of the outer wheel and hub to be the total stresses at standstill, shown in Figure 5-3. As shown in Figure 5-2, the tangential stress ( $S_t$ ) from the second shrink fit is in tension, reducing the compressive  $S_t$  from the first shrink fit.



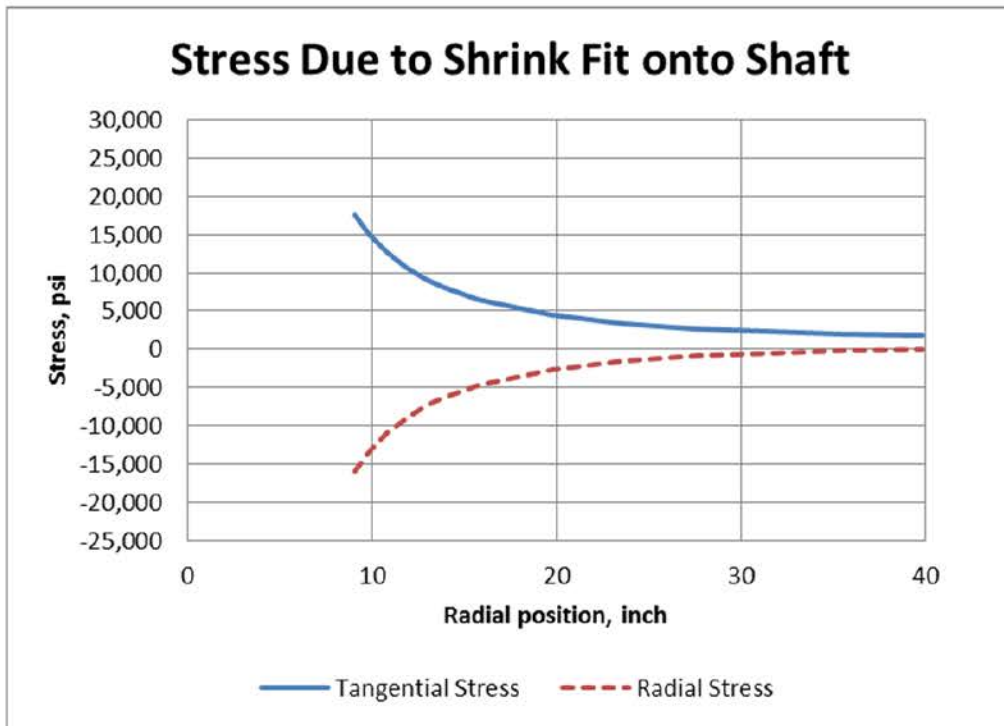


**Figure 5-2: Standstill Stress due to Shrink Fit onto Shaft**

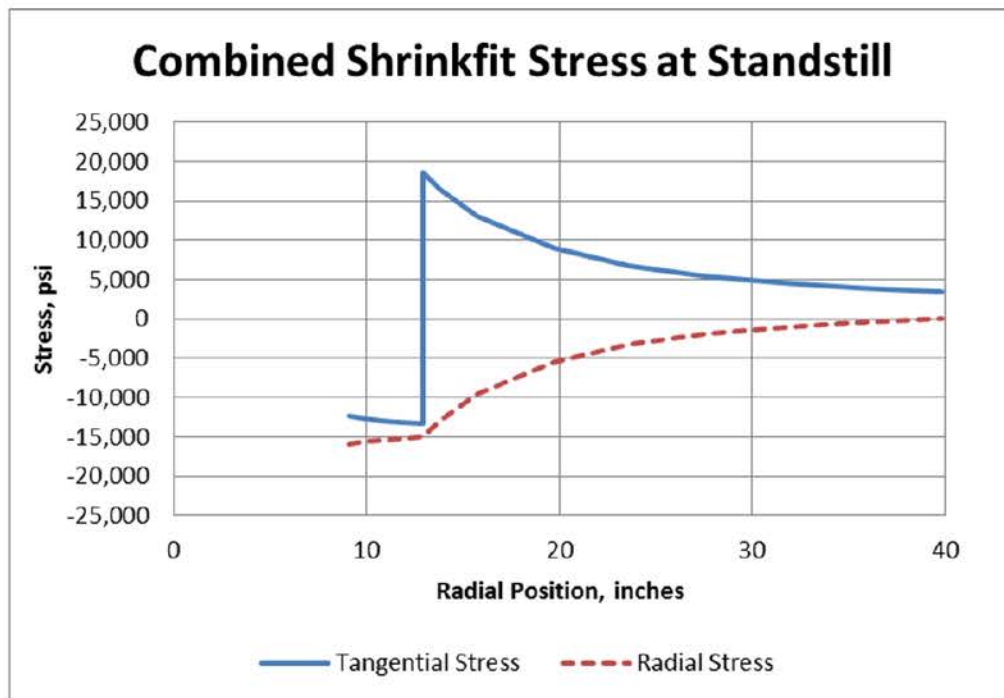


**Figure 5-3: Total Stress at Standstill**

The radial contact stress between the hub and the outer wheel is -15,012 psi.

The peak tangential (hoop) stress at the inside radius of the outer wheel is 18,524 psi.

## 5.6 STRESSES DUE TO ROTATION AT 1,200 RPM

The outer wheel, the hub and the shaft will rotate as a unit as long as there is a compressive radial stress at the boundary between the parts. The stress in the assembly due to rotation (Equations 9 and 10) will be combined with the shrink fit stress of the assembly. The rotation of the wheel assembly will reduce the contact stresses at the two shrink fit locations. This effect is captured by the rotation inertial radial stress calculated by Equation 10.

The tangential and radial stresses due to rotational inertia are determined from Equations 9 and 10, respectively. The inner radius is zero as the shaft is solid. These stresses are plotted for a rotation of 1,200 RPM in Figure 5-4.



**Figure 5-4: Stress due to Rotation at 1,200 RPM**

The total stress during operation at 1,200 RPM is the combination of the stress due to rotational inertia in Figure 5-4, and the stress due to shrink fit at standstill in Figure 5-3. The total stress is shown in Figure 5-5. This approach will result in a conservative estimate of the hoop stress, as it directly combines the standstill shrink fit tensile stresses with the tensile stresses from the rotation inertia.

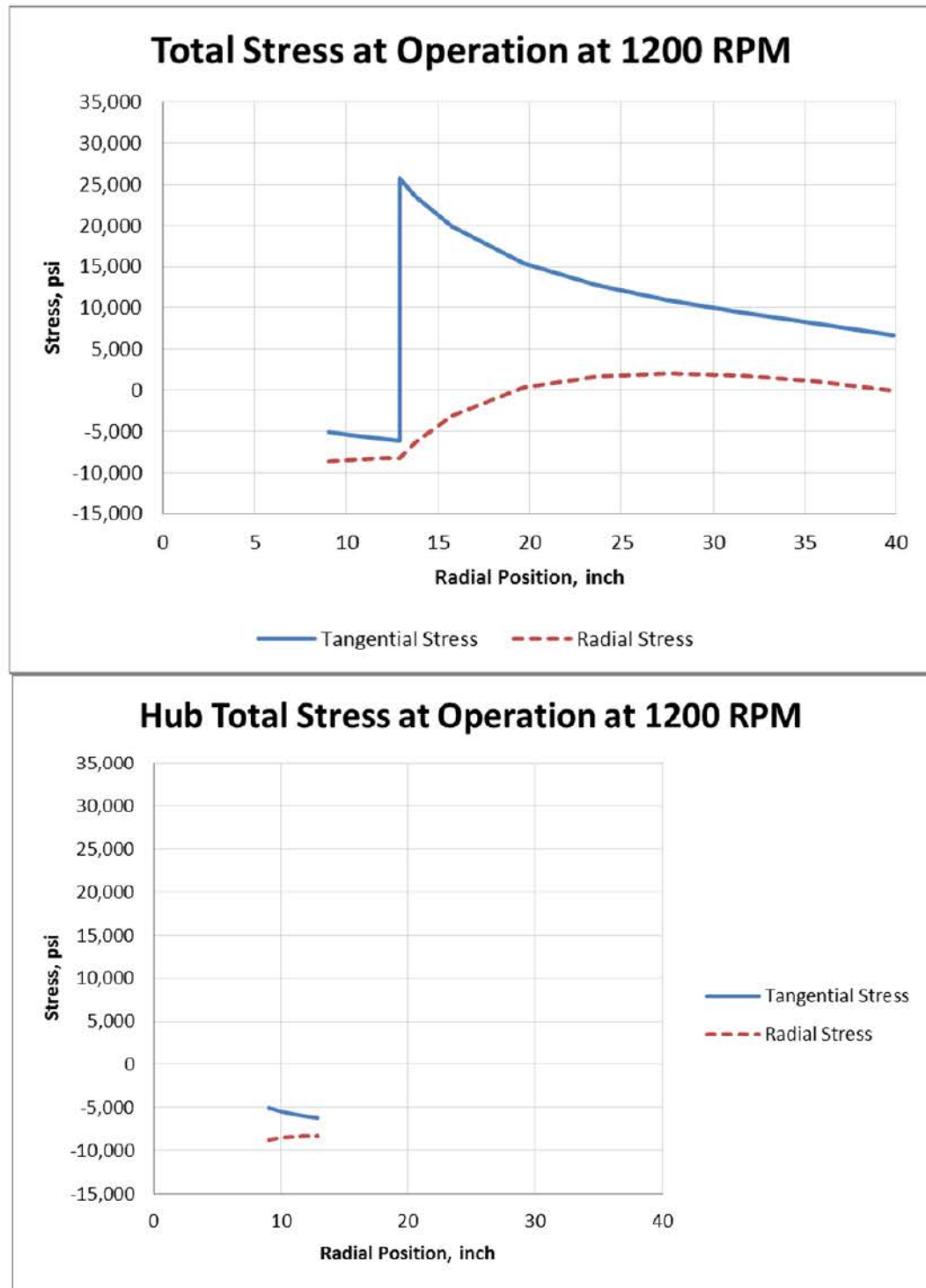


**Figure 5-5: Total Stress at 1,200 RPM**

The total radial stress between the hub and the outer wheel is -8,232 psi.

The peak tangential stress at the inside radius of the outer wheel is 25,640 psi.

The peak tangential stress at the inside radius of the hub is -5,055 psi.



## 5.7 STRESSES DUE TO ROTATION AT 125% OVER SPEED, 1,500 RPM

Using the same procedure and equations as used in the previous section, the stresses at operation at 1,500 RPM are computed. These stresses are shown in Figure 5-6. The total stress is always in compression for the entirety of the hub for overspeed at 1,500 RPM.

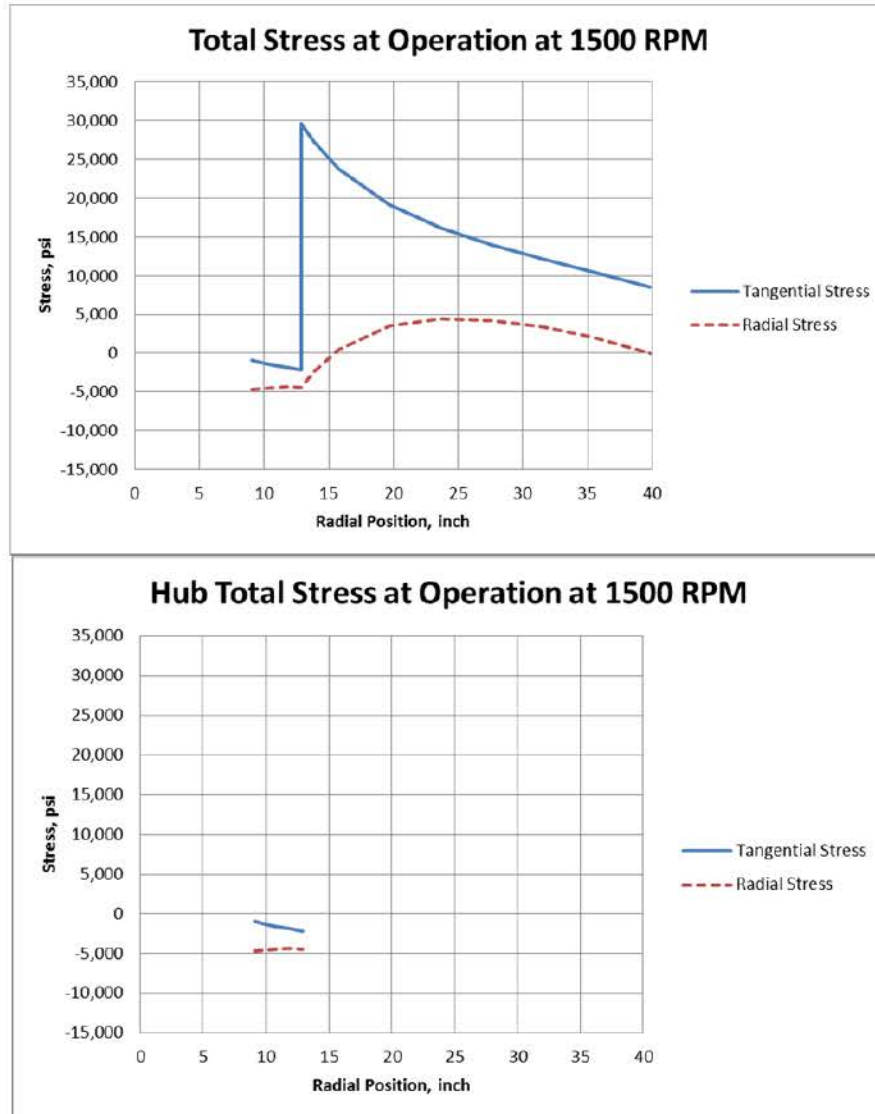


**Figure 5-6: Total Stress at Operation at 1,500 RPM**

The total radial stress between the hub and the outer wheel is -4,418 psi.

The peak tangential stress at the inside radius of the outer wheel is 29,644 psi.

## 5.8 STRESS DUE TO ROTATION AT 1,800 RPM

Since the joint release limit of 150% normal operation speed and stress requirement were removed from the specification [1], the stress calculation at 1,800 RPM is no longer relevant.

## 5.9 JOINT RELEASE SPEED FOR PRESCRIBED SHRINK VALUES

The joint release speed is obtained by iterating the speed until either the contact pressure between the wheel assembly and the shaft is zero, or until the contact pressure between the hub and the outer wheel is zero. The joint between the hub and outer wheel becomes loose at 1,786 RPM for the shrink fit values with the maximum tolerances. This results in the worst stress condition. The total stresses including the rotational inertia stress for 1,786 RPM are shown in Figure 5-7.

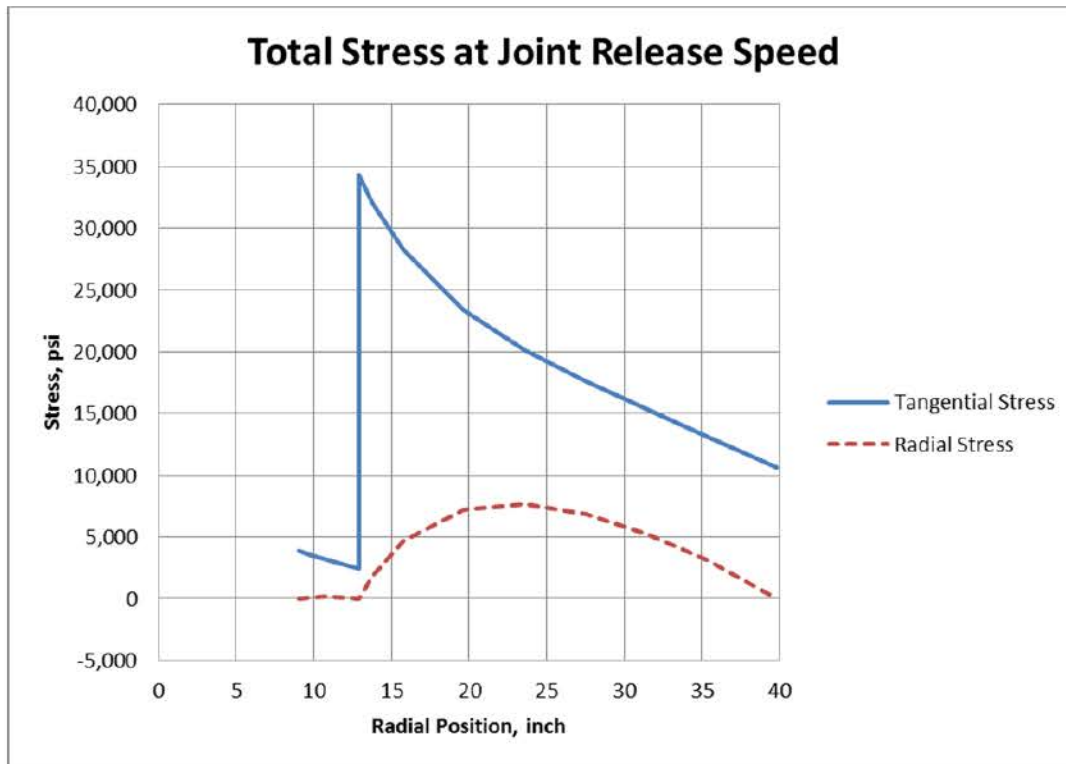


**Figure 5-7: Total Stresses at Joint Release Speed of 1,786 RPM**

The total radial contact stress at the hub and the outer wheel interface is 0 psi.

The peak tangential stress at the inside radius of the outer wheel is 34,280 psi.

The joint release speed was also calculated for the minimum tolerance, i.e., zero manufacturing tolerance and negative smoothing tolerance. The joint release speed is 1,662 RPM with the minimum tolerance.

## 5.10 CONSIDERATION OF MINIMUM SHRINK FIT

The optimized shrink fit values are recommended for the flywheel. Minimum shrink fit calculation prior to revision 3 of this report is no longer relevant.



## 5.11 EVALUATION OF STRESSES

Criterion 1: Total stress in the flywheel at normal operating speed shall not exceed  $1/3 S_y$ . The total stress for this application is defined as the von Mises stress, which is

$$[1/\sqrt{2}]*[(S_t - S_r)^2 + (S_t^2 + S_r^2)]^{1/2}.$$

The total von Mises stress at 1,200 RPM is 30,598 psi, which is less  $1/3$  than  $S_y = 30,941$  psi.

Criterion 2: Total stress at design overspeed shall not exceed  $2/3 S_y$ , where design overspeed is 125% of normal operating speed.

The maximum total von Mises stress at 125% of normal operation, 1,500 RPM = 32,081 psi, is less than  $2/3 S_y = 61,883$  psi.

φ

## 5.12 CONSIDERATION OF SEISMIC EVENT

The potential concern for seismic loads is a vertical (axial) force, which could exceed the friction resistance. (The friction resistance maintains the connection of the flywheel components.) The minimum friction forces at normal operation, the assumed starting point for a seismic event, would occur for the case of the minimum original shrink fit. Horizontal seismic acceleration has a negligible effect on the shrink fit of the flywheel assembly.

The hub-wheel radial contact stress is -8,232 psi at 1,200 RPM.

The hub-shaft radial contact stress is -8,713 psi at 1,200 RPM.

Assuming a coefficient of friction of 0.2, the total axial resistance to vertical movement of the flywheel assembly relative to the shaft is  $0.2 \times 8,713 \text{ psi} \times \text{thickness of the assembly} \times \text{circumference of the shaft}$  is 1,719,748 lbs.

The weight of the flywheel assembly is 23,174 lbs.

The ratio of the resistance friction force to the weight is the acceleration required to slip,  $A_{\text{slip}} = 1,719,748 / 23,174 = 74$  times gravity. This is significantly above the seismic requirement of three times gravity specified in [1].

Similarly, the radial contact stress between the hub and the outer wheel is -8,232 psi. The resistance friction force is 2,310,018 lbs. The acceleration required to slip is 100 times gravity. This is significantly above the seismic design requirement. Therefore, Criterion 3 is satisfied.

## 5.13 STRESS INTENSITY FACTOR OF CRACK FOR OUTER WHEEL

The stress intensity factor as a function of crack depth is computed from the stresses computed in the previous sections of this report. In all cases analyzed, the highest tensile stress is located on the inner radius of the outer wheel. The stress distribution from this point toward the outer edge of the wheel can be represented by the fourth order Equation 11, and the stress intensity factor,  $K_I$  due to this stress is computed using Equation 12. The calculated  $K_I$  at standstill, 1,200 RPM, 1,500 RPM and 1,786 RPM are compared to  $K_{IC}$  (150 ksi-in<sup>1/2</sup>) to ensure non-ductile fracture does not occur. Critical speed for non-ductile fracture is evaluated and discussed in Section 5.14. Note that since the hub is always in compression, only the outer wheel needs to be evaluated.



Outer Wheel  $K_I$  at Standstill

The tangential stress is taken from Figure 5-3. The stress as a function of the flaw depth to thickness ratio is fit to a fourth order polynomial in Figure 5-8.

The radial extent of the outer wheel from the inner to outer radius is [ ]<sup>a, c, e</sup>. The stress, in Equation 11 form, is:

$$S_t = S_0 + S_1(x/t) + S_2(x/t)^2 + S_3(x/t)^3 + S_4(x/t)^4$$

$$S_t = 18,415 - 61,531(x/t) + 120,122 (x/t)^2 - 116,469(x/t)^3 + 43,001(x/t)^4$$

Outer wheel  $K_I$  from Equation 12 is shown in Figure 5-9:

$$K_I = [G_0S_0 + G_1S_1(a/t) + G_2S_2(a/t)^2 + G_3S_3(a/t)^3 + G_4S_4(a/t)^4] \sqrt{(\pi a)}$$

In the previous equation:

a = crack length in radial direction

t = radial thickness of outer wheel

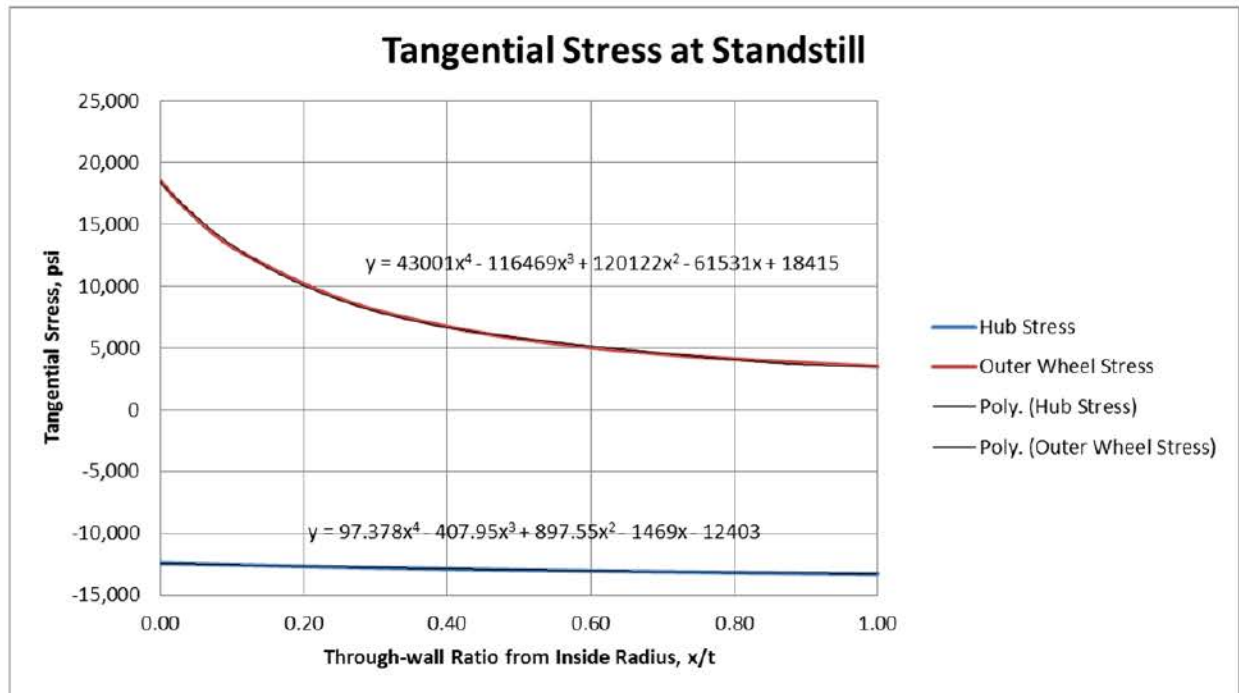


Figure 5-8: Polynomial Tangential Stress at Standstill

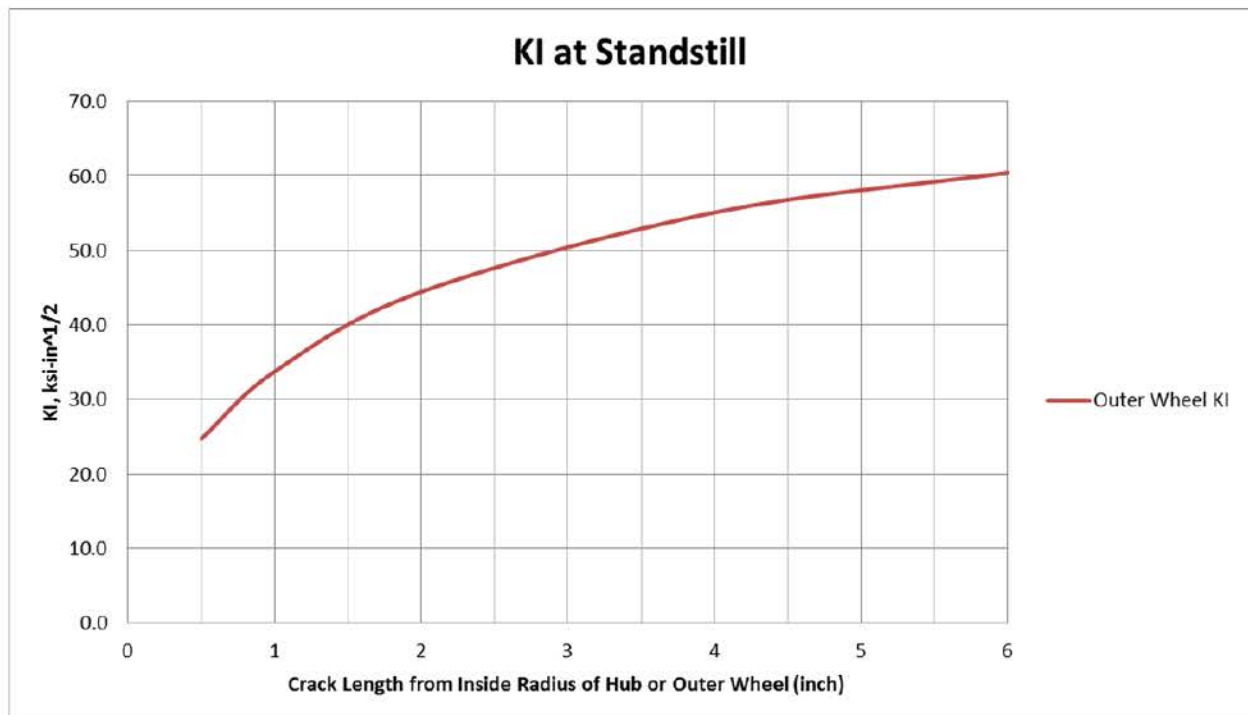
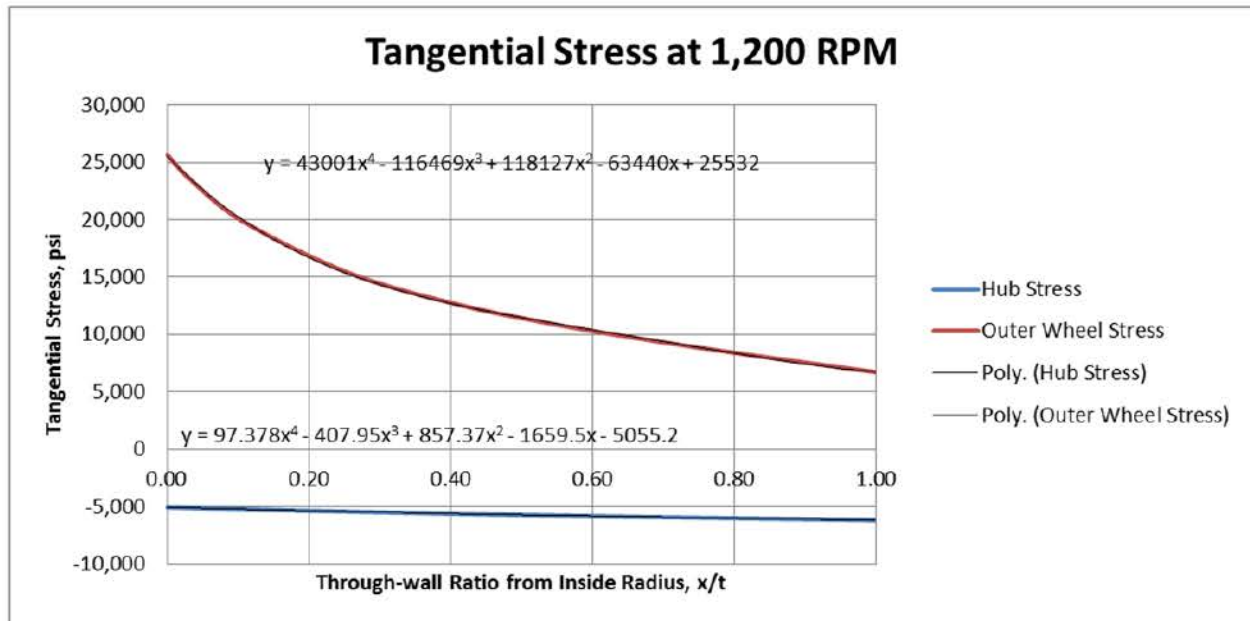


Figure 5-9: Stress Intensity Factor versus Crack Length at Standstill

$K_I$  at 1,200 RPM

The tangential stress is taken from Figure 5-5. The stress as a function of through-wall ratio of hub or outer wheel is fit to a fourth order polynomial in Figure 5-10.



**Figure 5-10: Polynomial Tangential Stress at 1,200 RPM**

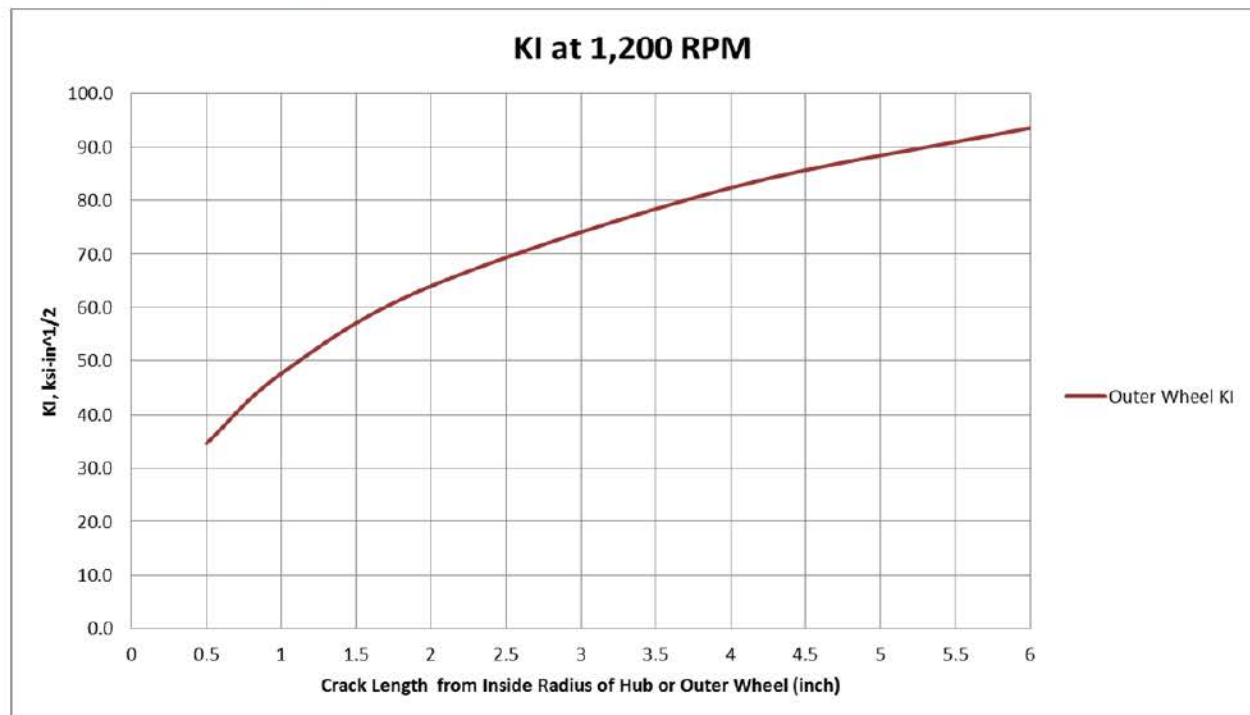


**Figure 5-11: Stress Intensity Factor versus Crack Length at 1,200 RPM**

The outer wheel location is bounding at 1,200 RPM. For a 0.5-inch crack,  $K_I = 34.6 \text{ ksi-in}^{1/2}$ . Therefore,  $K_{IC} / K_I = 4.33$ , and there is no risk of non-ductile fracture.



$K_I$  at 1,500 RPM

The tangential stress is taken from Figure 5-6. The stress as a function of through-wall ratio of hub or outer wheel is fit to a fourth order polynomial in Figure 5-12.

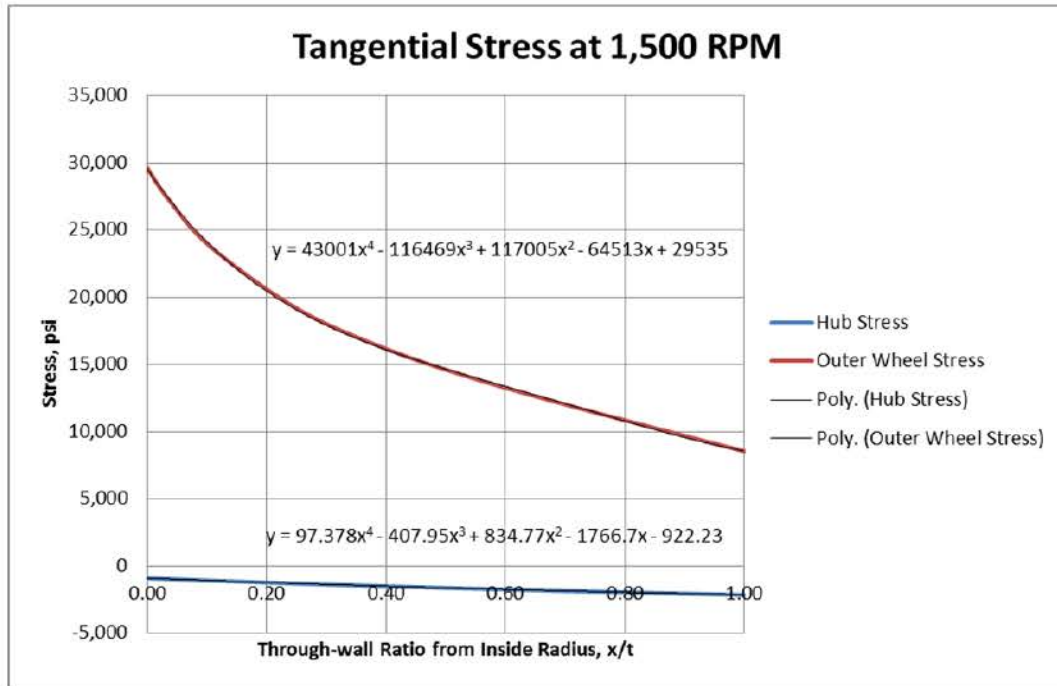


**Figure 5-12: Polynomial Tangential Stress at 1,500 RPM**

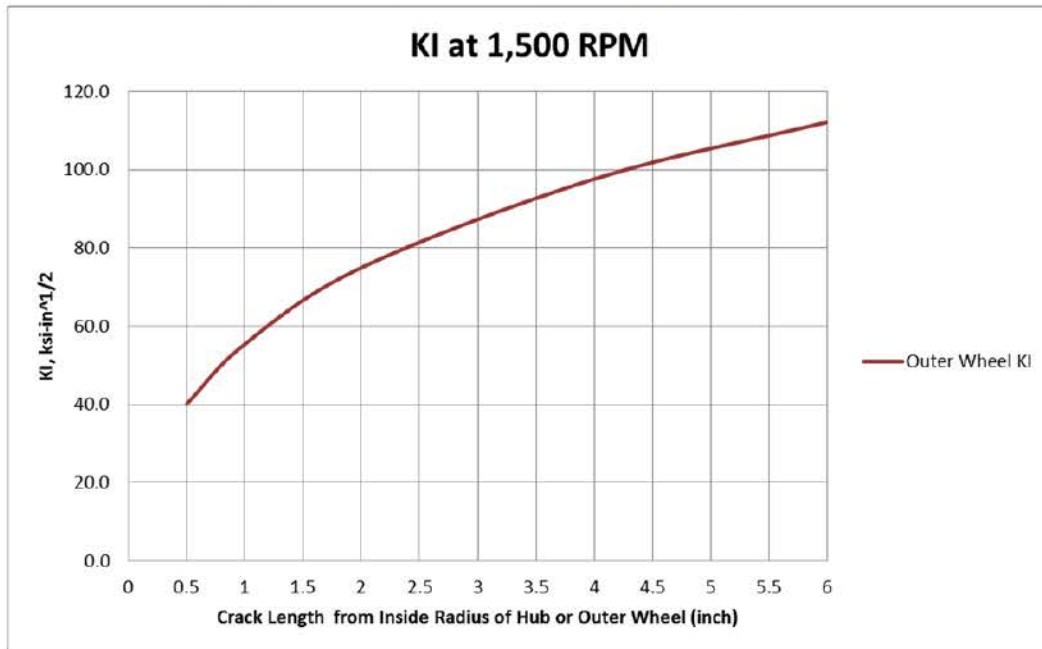


**Figure 5-13: Stress Intensity Factor versus Crack Length at 1,500 RPM**

The outer wheel location remains bounding for 1,500 RPM. For a 0.5-inch crack,  $K_I = 40.2 \text{ ksi-in}^{1/2}$ . Therefore,  $K_{IC} / K_I = 3.73$ , and there is no risk of non-ductile fracture.

## 5.14 EVALUATION OF INTEGRITY

**Criterion 4:** The critical speed for ductile fracture should be predicted.

The critical speed for ductile fracture can be conservatively estimated by determining the speed at which the maximum stress reached 0.7 times the ultimate stress. This criterion is consistent with ASME Code Section III, Article F-1330 [5].

Figure 5-7 shows that, at separation speed (1,786 RPM), the maximum tangential stress is 34,280 psi at the inside radius of the outer wheel.

Since the shrink fit stress is no longer present, the stress scales as the square of the rotation speed. Therefore, the speed at which the stress reaches  $0.7 S_u$  (81,221 psi) is calculated as follow:

$$(1,786 \text{ RPM})^2 : 34,280 \text{ psi} = (\text{critical RPM})^2 : 81,221 \text{ psi}$$

The ductile fracture critical RPM = 2,748.

**Criterion 5:** The critical speed for non-ductile fracture should be predicted. To predict the critical speed for non-ductile fracture, a crack size must be hypothesized. For conservatism, a crack length of 0.50 inches is evaluated. The rotation speed to reach the minimum  $K_{IC}$  of 150 ksi-in<sup>1/2</sup> is plotted in Figure 5-14 as a function of crack size.

The bounding critical speed for a crack length of 0.5 inches located at the inside radius of the outer wheel is 3,203 RPM.

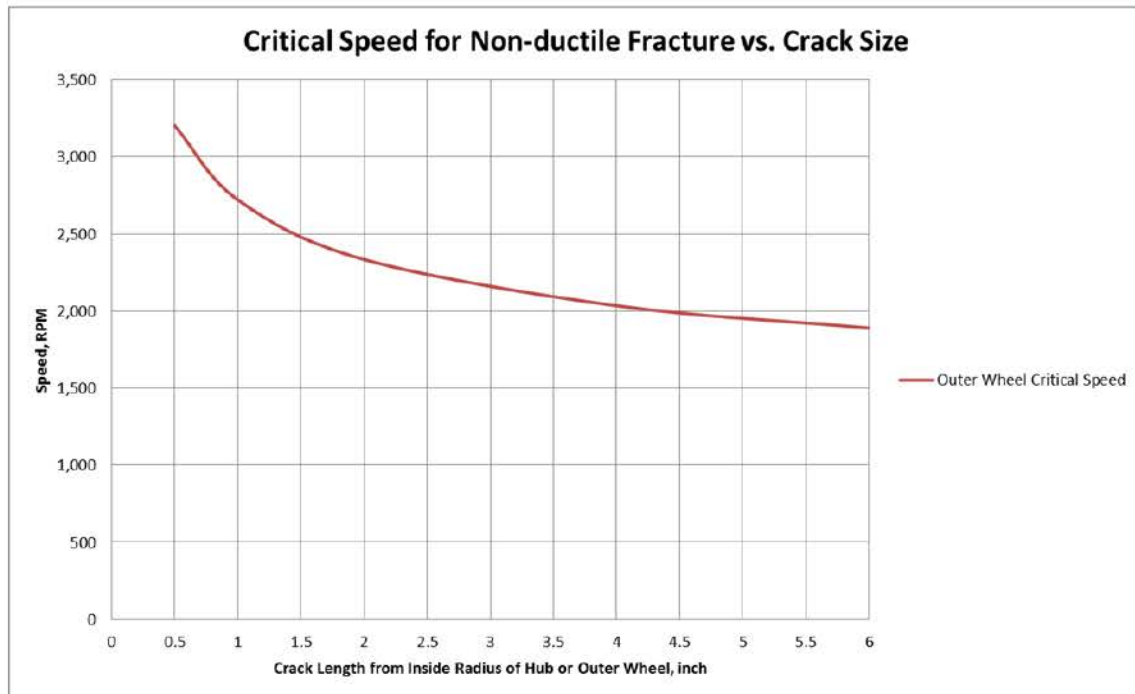


**Figure 5-14: Rotation Speed to Reach a  $K_{IC}$  of 150 ksi-in<sup>1/2</sup>**

**Criterion 6:** The normal speed should be less than one-half of the lowest critical speeds. As shown in Table 5-1, this criterion is satisfied.

**Table 5-1: Normal and Critical Speed Comparison**

Critical Speed	Speed (RPM)	Normal Operation Speed/Critical Speed Ratio	Critical Speed/Joint Separation Speed Ratio
Ductile Fracture	2,748	$0.44 < 0.5$ Per Criterion 7	1.54
Non-ductile Fracture	3,203	$0.37 < 0.5$ Per Criterion 7	1.79
Excessive Deformation	2,938	$0.41 < 0.5$ Per Criterion 7	1.65

Note: Since critical speeds are greater than the separation speed of 1,786 RPM, these critical speeds are only hypothetical, and could not occur in real life.

Criterion 7: The predicted LOCA overspeed should be less than the lowest critical speed.

The design overspeed is 125% of normal operation = 1,500 RPM. This is less than all critical speeds. This criterion is satisfied.

Criterion 8: The critical speed for excessive deformation of the flywheel should be predicted.

The critical speed for excessive deformation can be conservatively estimated by determining the speed at which the maximum stress reached the yield stress.

Figure 5-7 shows that, at separation speed of 1,786 RPM, the maximum tangential stress is 34,280 psi at the inside radius of the wheel. Since the shrink fit stress is no longer present, the stress scales as the square of the rotation speed. Therefore, the speed at which the stress reaches the yield stress (92,824 psi) is 2,938 RPM. Since this is greater than the joint separation speed, it is a hypothetical value that is impossible to be reached. Therefore, excessive deformation at overspeed conditions (i.e., 1,500 RPM) will not occur.

## 5.15 FATIGUE CRACK GROWTH

The fatigue crack growth due to a life time of 6,000 cycles from standstill to normal operation can be predicted by the fatigue crack growth rates available in [5]. The delta  $K_I$  from standstill to normal operation is determined by comparing the  $K_I$  in Figure 5-9 and Figure 5-11. The delta  $K_I$  for the outer wheel is shown in Figure 5-15.

Fatigue crack growth can be calculated using the generic carbon and low alloy ferritic steel growth rate in the ASME Section XI, Figure A-4300-1 in [5]:

$$da/dn = C_0 (\Delta K_I)^n$$

In the previous equation:

$$C_0 = 1.99 \times 10^{-10} \text{ S}$$

$$S = 25.72 \times (2.88 - R)^{-3.07}$$

$$n = -3.07$$

$$R = K_{Imin}/K_{Imax}$$



A crack grows from 0.5 inches to 0.5032 inches in 6,000 lifetime cycles from standstill to normal operation. This is negligible growth.

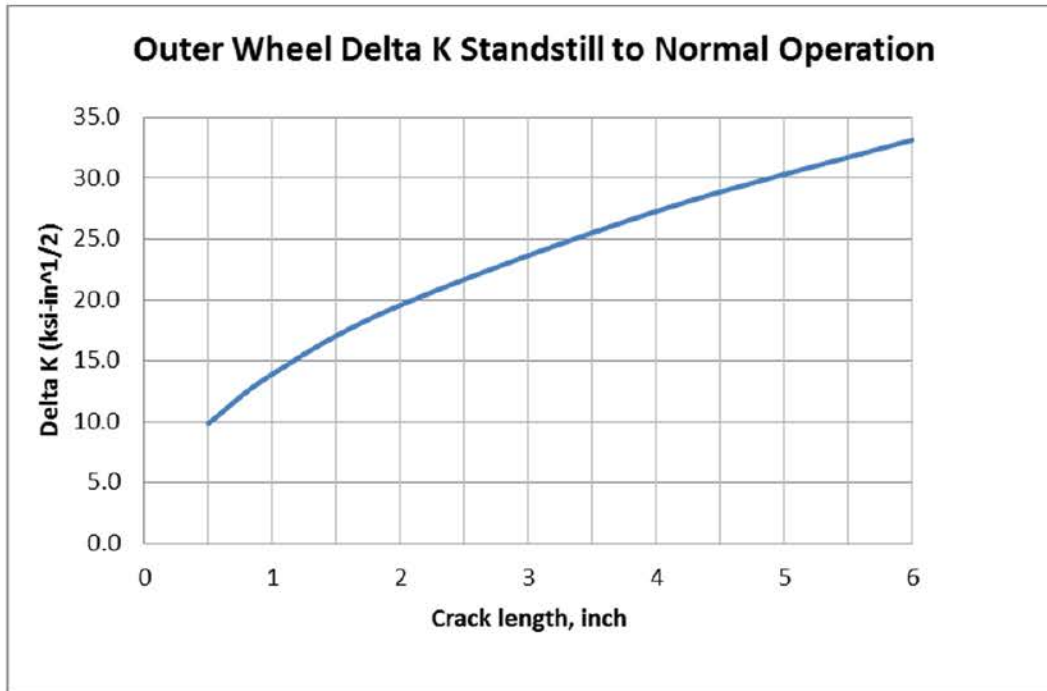


**Figure 5-15: Change in Outer Wheel  $K_I$  from Standstill to Normal Operation**

Since the hub is always in compression, as shown in Figure 5-3 and Figure 5-5, the fatigue crack growth for the hub is negligible.

## 6 RESULTS AND CONCLUSIONS

This report demonstrates that the APR1400 RCP flywheel satisfies all of the RCP flywheel integrity criteria of the design specification [1] and U.S. NRC Regulatory Guide 1.14 [2]:

The acceptance criteria in the specification [1] include:

1. The total stress 30,598 psi at normal operating speed does not exceed  $1/3 S_y$  of 30,941 psi. This criterion is met.
2. The total stress at design overspeed does not exceed  $2/3 S_y$ , where design overspeed is 125% of normal operating speed. This criterion is met. .

The Regulatory Guide acceptance criteria are established in [2] as:

3. Flywheel assembly is designed to withstand normal conditions, anticipated transients, the design basis loss of coolant accident (LOCA), and the safe shutdown earthquake without loss of structural integrity.
4. The critical speed for ductile fracture is 2,748 RPM.
5. The critical speed for non-ductile fracture is 3,203 RPM.
6. The normal speed is less than one-half of the lowest critical speeds for fracture. This criterion is met.
7. The LOCA overspeed of 1,500 RPM is less than the lowest critical speeds. This criterion is met.
8. Excessive deformation can be conservatively defined as total stress reaching material yield strength,  $S_y$ . The shrink fit release speed is 1,786 RPM, with a maximum stress of 34,280 psi. This is much less than the  $S_y$  of 92,824 psi. The hypothetical speed at  $S_y$  is 2,938 RPM, which will not occur because the shrink fit will separate at 1,786 RPM. Additionally, the separation speed of 1,786 RPM is significantly greater than the LOCA overspeed of 1,500 RPM. Consistent with past practice [7], the excessive deformation criterion is considered satisfied.

## 7 REFERENCES

1. KEPCO Design Specification, 11A60-FS-DS485, Rev. 05, "Design Specification for Reactor Coolant Pump Motors," June 5, 2017.
2. US Nuclear Regulatory Commission Regulatory Guide 1.14, Rev. 1, "Reactor Coolant Pump Flywheel Integrity," August 1975.
3. Young, Warren C. and Richard G. Budynas, "Roark's Formulas for Stress and Strain," Seventh Edition, McGraw-Hill Companies, Inc., New York, NY, 2002.
4. API 579-1/ASME FFS-1, "Fitness-For-Service," Annex C, "Compendium of Stress Intensity Factor Solutions," June 5, 2007.
5. ASME Boiler and Pressure Vessel Code, Section III, Division 1, Rules for Construction of Nuclear Facility Components, 2007 Edition with 2008 Addenda, Section XI, Appendix A 4300.
6. Siemens Document, 4D5.0170.83-575711F, Rev. F, "Flywheel Calculation," May 30, 2011.
7. Westinghouse Report, WCAP-15666-A, Rev. 1, "Extension of Reactor Coolant Pump Motor Flywheel Examination," October 2003.
8. U.S. Nuclear Regulatory Commission Report, NUREG-0800, "Standard Review Plan for the Review of Safety Analysis Reports for Nuclear Power Plants: LWR Edition (NUREG-0800, Formerly Issued as NUREG-75/087)," Section 5.4.1.1, Rev. 3, "Pump Flywheel Integrity (PWR)," May 2010.
9. Westinghouse Letter, LTR-MRCDA-16-98-P, Rev. 0, "Westinghouse Responses to NRC RAI 503-8641 on the APR1400 RCP Flywheel Integrity," September 14, 2016.